



Chemically modified polyurethane-SiO₂/TiO₂ hybrid composite film and its reusability for photocatalytic degradation of Acid Black 1 (AB 1) under UV light

K.P.O. Mahesh^a, Dong-Hau Kuo^{a,*}, Bo-Rong Huang^a, Masaki Ujihara^b, Toyoko Imae^b

^a Department of Materials Science and Engineering, National Taiwan University of Science and Technology, Taipei 10607, Taiwan

^b Graduate Institute of Applied Science and Technology, National Taiwan University of Science and Technology, Taipei 10607, Taiwan



ARTICLE INFO

Article history:

Received 19 November 2013

Received in revised form 17 January 2014

Accepted 18 January 2014

Available online 28 January 2014

Keywords:

Polyurethane

SiO₂ sphere

TiO₂ photocatalyst

SiO₂/TiO₂ composite sphere

Hybrid composite

Photocatalytic activity

ABSTRACT

In this work, we have immobilized the surface modified SiO₂ core/TiO₂ shell composite sphere into polyurethane (PU) matrix to control the leaching of SiO₂/TiO₂ composite sphere during the photodegradation of dye solution. The uniform particle shape and sizes of SiO₂ sphere and SiO₂/TiO₂ composite sphere are synthesized without aggregation by sol-gel method. The SiO₂/TiO₂ composite spheres are chemically bonded with polyurethane using glycidoxypropyltrimethoxy silane (GPTMS) as a coupling agent to increase the flexibility and reusability of the resulting PU-SiO₂/TiO₂ hybrid composite film for photocatalysis. The PU-SiO₂/TiO₂ hybrid film has been extensively characterized by FT-IR, XRD, TGA, FE-SEM and TEM. The sizes of the prepared SiO₂ sphere and SiO₂/TiO₂ composite are about 310 nm and 320 nm, respectively. Photocatalytic activity of PU-SiO₂/TiO₂ hybrid film was studied towards Acid Black 1 (AB 1) under UV irradiation. The effects of operational parameters such as the amount of SiO₂/TiO₂ photocatalyst and initial pH on photomineralization have been analyzed. PU-40 wt% SiO₂/TiO₂ hybrid film with only 2.6 wt% TiO₂ has achieved a very good photocatalytic activity and is reusable under cyclic tests.

© 2014 Elsevier B.V. All rights reserved.

1. Introduction

Heterogeneous photocatalysis has been extensively used for removing organic contaminants from aqueous or gaseous environment [1,2]. TiO₂ is one of the most important semiconductor materials, because it is easily available, inexpensive, non-toxic, and has potential applications in numerous fields, such as photocatalyst [3–6], sensors [7,8], solar cells [9,10], and lasers [11]. However, when TiO₂ is used as a single component, it has large band gap and high recombination rate of the photogenerated electron-hole pair that will reduce the complete utilization of UV and solar energy. The specific surface area of commercially available TiO₂ is about 60 m²/g. To increase the photocatalytic activity of TiO₂, it was coated on the surface of the SiO₂ nanosphere to form SiO₂/TiO₂ nanocomposite sphere. Even though SiO₂ falls in the category of insulator material, the photocatalytic activity of TiO₂ increased when combined with SiO₂ due to its large surface area [12,13]. Several researchers used SiO₂ nanoparticle to reduce the recombination of photogenerated electron-hole pair and to increase the

surface area of the TiO₂ photocatalyst for the purpose of improving the photodegradation ability of dyes [14–16].

If the SiO₂/TiO₂ powder is used as catalyst in the form of suspension, removal of catalyst after photodegradation requires a solid-liquid separation technique that consumes both money and time and the recovery loss of catalyst will be high. The floating of powder may affect the human health [17]. The separation of the floating catalyst from dye solution can be difficult. If the catalyst powder cannot be separated from the dispersion after photocatalytic testing, the concentration measurement of the degradable species by UV-vis spectra will be a problem. Moreover, reusability will also be affected by the catalyst lost during filtration or centrifugation.

To be a reusable photocatalyst, the photocatalytic powder needs to be embedded into a polymer matrix. The characteristic features of polymer support should control the leaching problem of catalyst, as well as the loss of catalyst during recovery. Moreover, polymer support is expected not to affect the specific surface area and activity of photocatalyst. Recently, many researchers have immobilized the TiO₂ photocatalyst in different polymers. Zhang and his group successfully dispersed TiO₂ in PMMA and PET by electrospun method to form the hydrogen bonding between TiO₂ precursors and PMMA matrix [18,19]. Yao et al. deposited TiO₂ nanoparticle on

* Corresponding author. Tel.: +886 2 2730 3291; fax: +886 2 2730 3291.

E-mail address: dhkuo@mail.ntust.edu.tw (D.-H. Kuo).

activated carbon fiber by sol–gel method and their photocatalytic effect is tested using phenol and methyl orange [20]. Matzusawa et al. had immobilized the TiO₂ nanoparticles through the physico-chemical interaction on the nonwoven polyester fibers coated with the SiO₂/PVC-PVA copolymer hybrid layer [21]. Hosseini et al. used highly porous perlite granules as adsorbent to adsorb TiO₂ nanoparticles into its pores and studied their photocatalytic activity using phenol as a pollutant [22]. Recently, Lei et al. immobilized the TiO₂ nanoparticle only upto 12 wt% into the polyvinyl alcohol (PVA) with hydrogen bonding [23]. In all these cases, TiO₂ nanoparticle has been used and is not chemically bonded with polymer substrate or matrix. Thus, the leaching of TiO₂ particles can be a problem, which affects the reusability of catalyst. Furthermore, they could not have high loading of TiO₂ nanoparticles into the polymer matrix due to the formation of high viscous polymer solution that will affect the film-making process. Chemical bonding between TiO₂ and polymer matrix can improve the leaching problem. Li et al. used γ -aminopropyltriethoxysilane to modify the surface of TiO₂ nanoparticle followed by covering a dense conductive PANI layer to form a PANI-coated TiO₂ through surface oxidative graft polymerization [24]. Yuranova et al. reported the photocatalytic activity of SiO₂/TiO₂ coated cotton textile. They have achieved the high CO₂ evolution during the discoloration of red wine by having the amount of SiO₂/TiO₂ higher than that of TiO₂ coated on cotton textile [25]. They used hybrid particle for photocatalytic testing, but they did not mention the loss of catalyst during the centrifugation. The use of polymer/TiO₂ hybrid film always has an existing problem in the passivation of TiO₂ nanoparticles by the polymer matrix. Without exposing TiO₂ to environment, its photocatalytic ability can be limited.

Nowadays, organic dyes are one of the foremost groups of pollutants found in wastewaters fashioned from different industries. Among azo dyes used in textile industry, Acid Black 1 (AB 1) is one of the frequently used dyes in textile industries and is a potential threat to the aquatic environment due to its poor biodegradability [26,27]. Recently, Swaminathan and their group reported the photocatalytic degradation of AB 1 by differently modified photocatalysts in slurry forms [28–31].

In the present work, uniform SiO₂ sphere of 310 nm in size was first prepared and TiO₂ was coated on the surface of the SiO₂ sphere to form the SiO₂/nano-TiO₂ composite sphere with the size of about 320 nm. The formed composite sphere was chemically modified through silane coupling agent followed by reacting with flexible polyurethane (PU) prepolymer to form PU-SiO₂/TiO₂ hybrid composite without particle aggregation. The surface morphologies of SiO₂/TiO₂ composite sphere and PU-SiO₂/TiO₂ hybrid composite film were studied by using TEM and FE-SEM and the photocatalytic activity of prepared hybrid composites was tested toward the degradation of Acid Black 1 (AB 1) dye.

2. Experimental

2.1. Materials

In this study, analytical grade chemicals were used as received without further purification. Polyurethane prepolymer (PU) (W-2907-05) was kindly supplied by Chemtura Corporation, Middlebury, Connecticut, USA. The AB 1 dye (Empirical formula: C₂₂H₁₄N₆Na₂O₉S₂) obtained from Aldrich was used as received. The chemical structure is presented in Figure S1 of the Supporting Information.

2.2. Synthesis of SiO₂ sphere

A mixture of 2 mL TEOS, 0.6 mL dodecane, 10 mL anhydrous ethanol, and 2 mL of water was stirred at room temperature for

30 min followed by addition of 0.4 mL of ammonia solution and continued the stirring for 10 min. Then add 6 mL of anhydrous ethanol to this mixture and continued the stirring for 2 h at room temperature, the SiO₂ spheres were separated by centrifugation and washed three times with ethanol. Finally, the SiO₂ sphere was dried under vacuum oven at 60 °C for 6 h.

2.3. TiO₂ coating on SiO₂ sphere

The SiO₂ sphere (1 g) dispersed in anhydrous 2-propanol (50 mL) was ultrasonicated for 30 min. To this, 0.5 mL of Ti(iOBu)₄, 0.2 mL of dodecane, and 0.1 mL of water was added and stirred for 4 h at room temperature. The TiO₂-coated SiO₂ spheres were separated by centrifugation and washed three times with ethanol and dried in vacuum oven at 60 °C for 6 h. The SiO₂/TiO₂ composite sphere was calcined at 450 °C for 4 h to get the anatase phase for TiO₂. The total amount of TiO₂ nanoparticle coated on the SiO₂ porous sphere was 4 wt%. The schematic diagram for the TiO₂ coating procedure to form SiO₂/TiO₂ sphere is shown in Scheme 1.

2.4. Surface modification of SiO₂/TiO₂ sphere

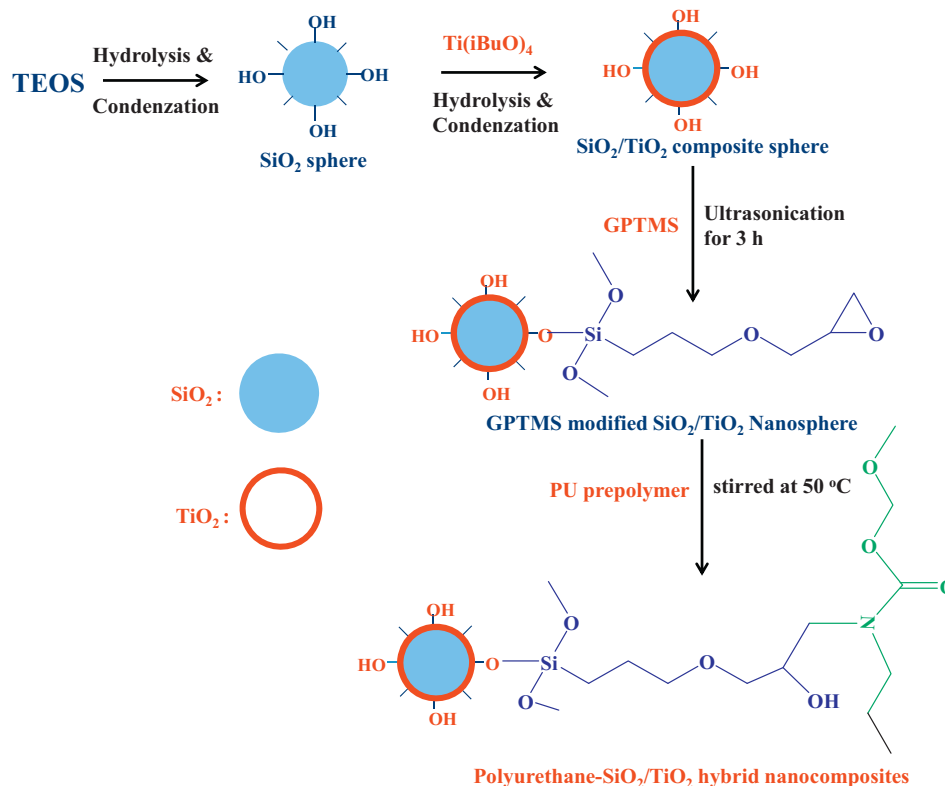
The SiO₂/TiO₂ sphere (40 mg) and ethanol (4 mL) was ultrasonicated for 30 min followed by adding glycidoxypropyltrimethoxy silane (GPTMS, 40 mg) to this solution. After 4 h ultrasonication, the unreacted GPTMS was removed by centrifugation. The GPTMS-modified SiO₂/TiO₂ sphere was further washed three times with ethanol to completely remove the unreacted GPTMS then re-dispersed in 4 mL THF under ultrasonication. The schematic diagram for the GPTMS-modified SiO₂/TiO₂ composite sphere is shown in Scheme 1.

2.5. Preparation of PU-SiO₂/TiO₂ hybrid film

Three different concentrations i.e., 25, 50 and 75 wt% of GPTMS-modified SiO₂/TiO₂ spheres were dispersed in THF and respective amount of PU prepolymer was added into the above solutions. The reaction mixture was stirred at 50 °C for 3 h. The solution of PU-SiO₂/TiO₂ hybrid was poured into petri-dishes and dried in a hot air oven at 50 °C for 6 h. The prepared PU-SiO₂/TiO₂ hybrid film was kept in a vacuum oven at 60 °C for 12 h to remove the solvent. The reaction of GPTMS-modified SiO₂/TiO₂ with polyurethane is also given in Scheme 1.

2.6. Characterizations

The surface modification of SiO₂/TiO₂ by GPTMS was confirmed by Fourier Transform Infrared Spectrometer (FT-IR) (FTS-1000; Digilab, Holliston, MA, USA). Surface morphologies of the SiO₂ and SiO₂/TiO₂ spheres were examined by a transmission electron microscope (TEM, H-7000, equipped with a CCD camera, Hitachi, Tokyo, Japan) and the cross-sectional view of PU-SiO₂/TiO₂ hybrid film by a field-emission scanning electron microscope (FE-SEM, JSM 6500F, JEOL, Tokyo, Japan). Powder X-ray diffraction (XRD) patterns were recorded with a Bruker D2-phaser diffractometer using CuK α radiation ($\lambda = 1.5418 \text{ \AA}$). The weight losses of PU and its composites were analyzed using a thermogravimetric analyzer (TA Instrument Q500, New Castle, DE, USA) at a heating rate of 10 °C min⁻¹ up to 600 °C in air. UV-vis diffuse reflectance spectra were recorded on Shimadzu UV-2450 UV-visible spectrophotometer equipped with an integrated sphere assembly using BaSO₄ as a reflectance sample. The degradation of AB 1 dye was monitored by Jasco V-670 UV spectrophotometer.

**Scheme 1.** Fabrication of polyurethane- $\text{SiO}_2/\text{TiO}_2$ hybrid composite.

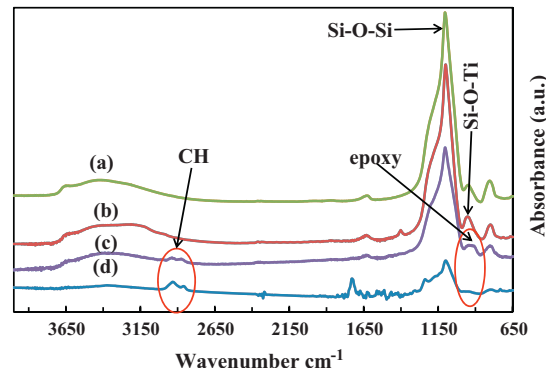
2.7. Photodegradation experiments

Photocatalytic activity of the prepared composite films was evaluated for its ability of photodegradation of AB 1 under UV irradiation using HOYA-SCHOTT Ex 250 photoreactor with UV light source <400 nm. In each experiment, AB 1 in an aqueous solution had an initial concentration of 10 ppm and the total weight of the PU- $\text{SiO}_2/\text{TiO}_2$ film photocatalyst was 160 mg. To ensure the adsorption and desorption equilibrium between film photocatalyst and AB 1 dye, the reaction solutions were kept in the dark with stirring for 30 min. Then the reaction solution was exposed to the UV light irradiation, 5 mL of aliquots were sampled out at a different irradiation time intervals and the concentration of AB1 was monitored by UV absorbance intensity at 615 nm.

3. Results and discussion

3.1. Characterization of catalyst

Surface modification is essential to disperse inorganic particle into polymer matrix without aggregation. In this study, we have modified the surface of $\text{SiO}_2/\text{TiO}_2$ by GPTMS coupling agent. The covalent bond formed between surface hydroxyl group of $\text{SiO}_2/\text{TiO}_2$ composite sphere and methoxy group of GPTMS. The surface modified $\text{SiO}_2/\text{TiO}_2$ composite reacts with PU through epoxy group of GPTMS. The oxirene ring in the epoxy (present in GPTMS-modified $\text{SiO}_2/\text{TiO}_2$ composite) was cleaved by secondary amino group of polyurethane prepolymer as shown in the Scheme 1. The methoxy groups in the GPTMS involved the hydrolysis and condensation reaction with hydroxyl groups on the surface of $\text{SiO}_2/\text{TiO}_2$ nanosphere. Fig. 1 shows the FT-IR spectra of (a) SiO_2 sphere, (b) $\text{SiO}_2/\text{TiO}_2$ composite sphere, (c) GPTMS-modified $\text{SiO}_2/\text{TiO}_2$ composite sphere, and (d) PU- $\text{SiO}_2/\text{TiO}_2$ hybrid composite film. The peaks observed at 1095 and 925 cm^{-1} confirmed the formation of

**Fig. 1.** FT-IR spectra of (a) SiO_2 sphere, (b) $\text{SiO}_2/\text{TiO}_2$ composite sphere and (c) GPTMS-modified $\text{SiO}_2/\text{TiO}_2$ composite sphere and (d) PU-40% $\text{SiO}_2/\text{TiO}_2$ hybrid composite film.

$\text{Si}-\text{O}-\text{Si}$ and $\text{Si}-\text{O}-\text{Ti}$ bands in SiO_2 sphere and $\text{SiO}_2/\text{TiO}_2$ composite sphere, respectively. The GPTMS-modified $\text{SiO}_2/\text{TiO}_2$ sphere showed the peaks at 3089 and 2930 cm^{-1} corresponding to the stretching vibrations of CH_2 in the GPTMS-modified $\text{SiO}_2/\text{TiO}_2$ sphere and PU- $\text{SiO}_2/\text{TiO}_2$ hybrid composite film. In addition, the appearance of the peak at 910 cm^{-1} indicated the presence of epoxy which confirms the presence of GPTMS on the $\text{SiO}_2/\text{TiO}_2$ particle as shown in Fig. 1(c). The disappearance of peak at 910 cm^{-1} is related to the cleavage of epoxy rings by amine groups in the polyurethane prepolymer as shown in Fig. 1(d).

Fig. 2 shows the XRD patterns of SiO_2 sphere, TiO_2 nanoparticle, and $\text{TiO}_2/\text{SiO}_2$ composite sphere. SiO_2 sphere is in an amorphous state and TiO_2 is in an anatase phase. After calcination of $\text{SiO}_2/\text{TiO}_2$ sphere at 450 °C for 4 h, all of the recorded peaks in the XRD patterns were indexed to the anatase phase of TiO_2 . The PXRD profile

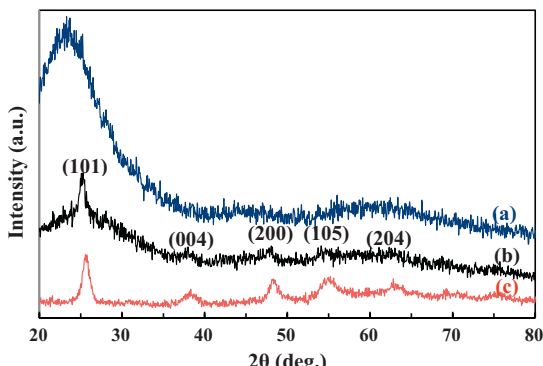


Fig. 2. XRD pattern of (a) SiO_2 nanosphere, (b) TiO_2 nanoparticle, and (c) $\text{SiO}_2/\text{TiO}_2$ hybrid composite sphere.

observed for $\text{SiO}_2/\text{TiO}_2$ composite sphere was agreed well with the reference profile (JCPDS 21-1272) of TiO_2 [12].

The SiO_2 sphere and $\text{SiO}_2/\text{TiO}_2$ composite sphere are prepared by sol-gel method followed by calcination at 450°C for 4 h. Fig. 3 shows the TEM images of monodispersed SiO_2 and $\text{SiO}_2/\text{TiO}_2$ composite sphere with fairly uniform particle size after calcination at 450°C for 4 h. The particle size of SiO_2 sphere is about 310 nm with very smooth surface. All the particles are not attached together and they are loosely spread on the surface. After TiO_2 being coated on SiO_2 , the size of the $\text{SiO}_2/\text{TiO}_2$ sphere is increased to 320 nm with rough surface as shown in Figs. 3(c) and (d). The TiO_2 shell on the SiO_2 sphere was not collapsed and not formed the large aggregates even after annealed at 450°C for 4 h. During the preparation of SiO_2 sphere, dodecane helped to make pores inside SiO_2 spheres and it acted as a foundation pit to strongly hold TiO_2 . Initially, the hydrolyzed TiO_2 sol filled the pores followed by condensation

reaction with hydroxyl groups to form $\text{Si}—\text{O}—\text{Ti}$ chain and TiO_2 grow on the whole SiO_2 surface to get uniform and much stable $\text{SiO}_2/\text{TiO}_2$ sphere.

Fig. 4(a) shows the cross-sectional FE-SEM image of PU-40% $\text{SiO}_2/\text{TiO}_2$ hybrid film. The $\text{SiO}_2/\text{TiO}_2$ spheres dispersed uniformly in the PU matrix and a thin PU layer were coated on the composite particles. There are no aggregates formed in the PU matrix though 40 wt% of $\text{SiO}_2/\text{TiO}_2$ sphere is incorporated into the PU matrix. The reason for the good dispersion is that GPTMS-modified $\text{SiO}_2/\text{TiO}_2$ sphere is chemically bonded with amine group of PU prepolymer as shown in Scheme 1. The presence of TiO_2 in $\text{SiO}_2/\text{TiO}_2$ sphere was also confirmed by FT-IR spectra and EDS analysis, as shown in Figs. 1 and 4(b), respectively. The peaks of EDS spectra obtained for the Si, Ti, and O atoms further confirmed the presence of Ti constituent in $\text{SiO}_2/\text{TiO}_2$ composite sphere (Fig. 4(b)). The Si/Ti atomic ratio present in the $\text{SiO}_2/\text{TiO}_2$ composite sphere was estimated by EDX spectra. The EDX results showed that the atomic ratio between Si and Ti was 96/4.

Fig. 5 shows the TGA thermograms of PU film and PU- $\text{SiO}_2/\text{TiO}_2$ hybrid films with different concentrations of $\text{SiO}_2/\text{TiO}_2$ composite spheres. TGA thermograms of all the hybrid composite films showed the similar thermal degradation behavior. The thermal stability of PU film increased with increasing the concentration of $\text{SiO}_2/\text{TiO}_2$ sphere in PU- $\text{SiO}_2/\text{TiO}_2$ hybrid composite film. Thermal degradation temperature of PU starts from 250°C and ends at 405°C whereas PU-70% $\text{SiO}_2/\text{TiO}_2$ hybrid film shows 260 and 425°C , respectively. From the TGA thermograms, we could confirm the actual amount of PU and $\text{SiO}_2/\text{TiO}_2$ sphere present in the PU- $\text{SiO}_2/\text{TiO}_2$ hybrid film. The contents of $\text{SiO}_2/\text{TiO}_2$ sphere in PU matrix are estimated as 20 wt% for PU (75 wt%)- $\text{SiO}_2/\text{TiO}_2$ (25 wt%), 40 wt% for PU (50 wt%)- $\text{SiO}_2/\text{TiO}_2$ (50 wt%) and 70 wt% for PU (25 wt%)- $\text{SiO}_2/\text{TiO}_2$ (75 wt%) hybrid composite film. The hybrid films are now presented as PU-20% $\text{SiO}_2/\text{TiO}_2$, PU-40% $\text{SiO}_2/\text{TiO}_2$, and PU-70% $\text{SiO}_2/\text{TiO}_2$.

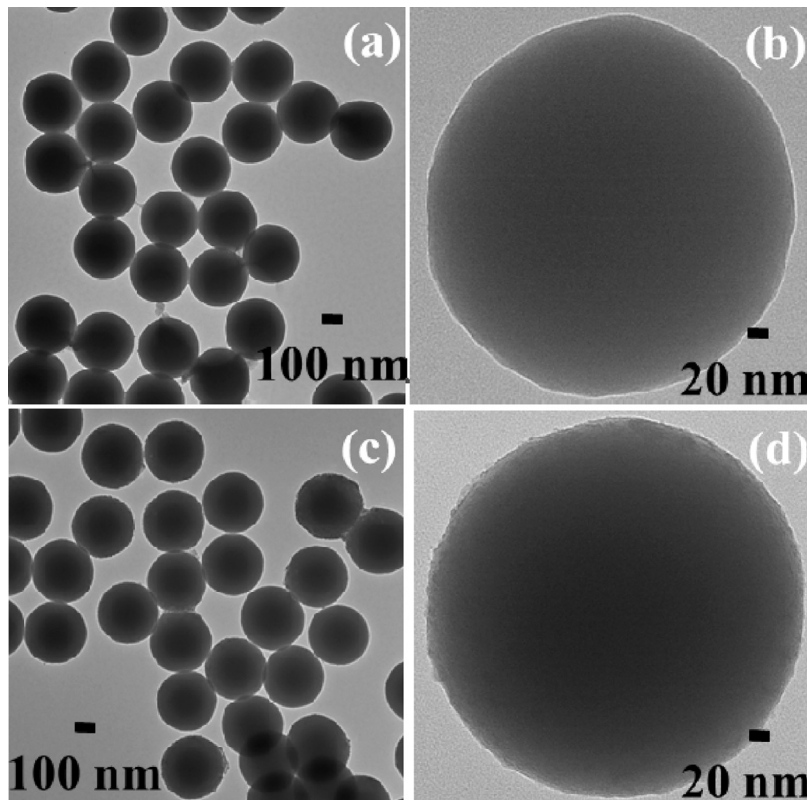


Fig. 3. TEM images of (a, b) SiO_2 sphere and (c, d) $\text{SiO}_2/\text{TiO}_2$ composite sphere at different magnifications.

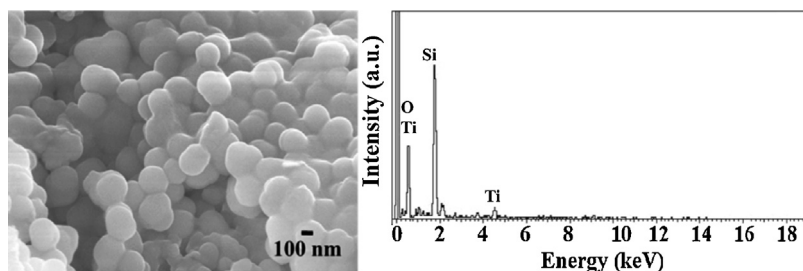


Fig. 4. (a) Cross-sectional FE-SEM image of PU-40% $\text{SiO}_2/\text{TiO}_2$ hybrid composite film and (b) EDX spectrum of the $\text{SiO}_2/\text{TiO}_2$ composite sphere.

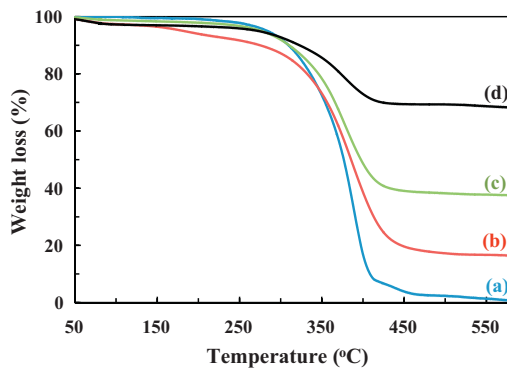


Fig. 5. TGA thermograms of (a) PU film and (b) 20 wt%, (c) 40 wt%, and (d) 70 wt% $\text{SiO}_2/\text{TiO}_2$ composite sphere-incorporated PU films.

UV-vis diffuse reflectance spectra of the SiO_2 sphere and $\text{SiO}_2/\text{TiO}_2$ composite sphere are shown in Fig. 6. $\text{SiO}_2/\text{TiO}_2$ composite sphere shows a strong absorption only in the ultraviolet region of 200–400 nm that indicates more photocatalytic activity in the UV region whereas there is no absorption observed in the both UV and visible region for SiO_2 composite sphere.

3.2. Photocatalytic degradation of AB 1 dye

Acid Black 1 (AB 1) dye was used as a pollutant to study the photocatalytic activity of PU- $\text{SiO}_2/\text{TiO}_2$ hybrid composite films. The thickness and weight of the hybrid composite film were 200 μm and 160 mg, respectively. The amount of TiO_2 was calculated based on the EDX and TGA results. 160 mg of PU-20% $\text{SiO}_2/\text{TiO}_2$ hybrid composite film contains 32 mg of $\text{SiO}_2/\text{TiO}_2$ sphere with SiO_2 of 30.7 mg and TiO_2 of 1.3 mg as per EDS results of 4 wt% TiO_2 present on the SiO_2 sphere. Based on the above calculation, we could calculate for PU-40% $\text{SiO}_2/\text{TiO}_2$ and PU-70% $\text{SiO}_2/\text{TiO}_2$ hybrid composite films as 2.6 and 4.6 mg of TiO_2 nanoparticles deposited on the SiO_2 spheres, respectively.

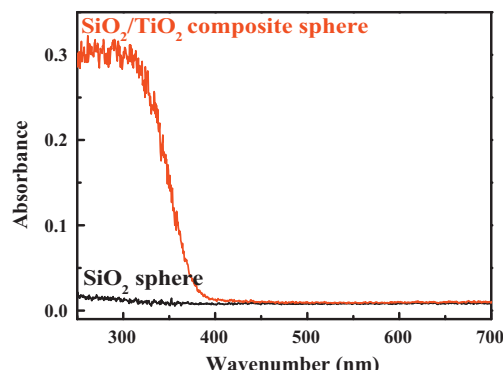


Fig. 6. UV-vis DRS of SiO_2 sphere and $\text{SiO}_2/\text{TiO}_2$ composite sphere.

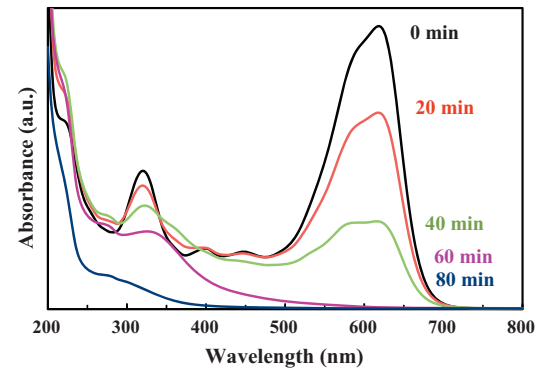


Fig. 7. Changes in UV-vis spectra of AB 1 dye on UV irradiation in the presence of PU-40% $\text{SiO}_2/\text{TiO}_2$ hybrid composite film at pH 6.5.

Fig. 7 shows the UV-vis spectra of AB 1 aqueous solution in the presence of PU-40% $\text{SiO}_2/\text{TiO}_2$ hybrid film with different irradiation time. There is no significant change in the peak positions of UV-vis spectra during irradiation, whereas the intensities observed at 320 nm and 615 nm decreased gradually with increasing the irradiation time that confirms the degradation of AB 1 dye. When the PU- $\text{SiO}_2/\text{TiO}_2$ hybrid film was immersed into the dye solution, the swelling of film is observed and the color of the film becomes pale blue. After completion of the photodegradation, the film retained the original color that confirms the dye solution was completely discolored by catalyst during the photo reaction. It could be understood that the hybrid film not only absorbs the dye but also absorbs dye solution in its free volume during swelling. When the dye solution was absorbed by hybrid film, the solution is very close to $\text{SiO}_2/\text{TiO}_2$ sphere and the degradation of AB 1 dye under UV irradiation become easily accessible.

3.3. Effect of catalyst loading in PU film

The effect of concentration of $\text{SiO}_2/\text{TiO}_2$ sphere in PU- $\text{SiO}_2/\text{TiO}_2$ hybrid film on the degradation of AB 1 dye has been investigated using three different concentrations of $\text{SiO}_2/\text{TiO}_2$ spheres, i.e., 20, 40 and 70 wt% in PU matrix, as shown in Fig. 8. It was observed that 100% discoloration had been achieved for all the samples within 80 min irradiation except for pure PU and without catalyst. In absence of either UV or catalyst, the AB 1 dye could not degrade even 1% for 80 min irradiation because AB 1 dye is resist to self-photolysis [28–31]. The photocatalytic activity increased to a maximum as the $\text{SiO}_2/\text{TiO}_2$ sphere loading in PU- $\text{SiO}_2/\text{TiO}_2$ film catalyst reached to 40 wt%. Further increasing the concentration of $\text{SiO}_2/\text{TiO}_2$ sphere decreased its ability in the degradation of AB 1 dye (Fig. 8). The reason for increasing the rate of dye degradation is attributed to the higher amount of catalyst sphere that could increases the rate of degradation of dye molecules as well as more catalyst particles exposed to the UV illumination. The decrease in the photo-induced degradation for the high $\text{SiO}_2/\text{TiO}_2$ sphere

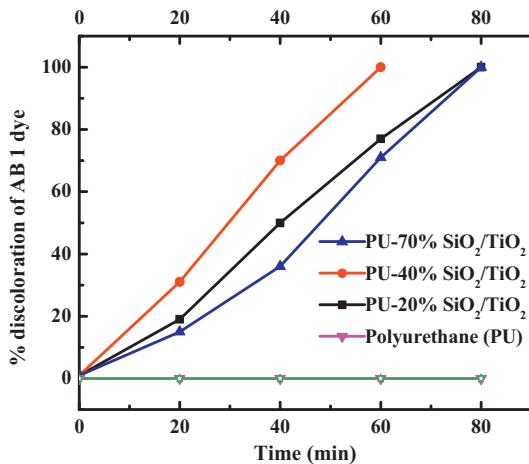


Fig. 8. Photodegradation of AB 1 dye with different concentrations of SiO₂/TiO₂ composite sphere in PU-40% SiO₂/TiO₂ hybrid composite film.

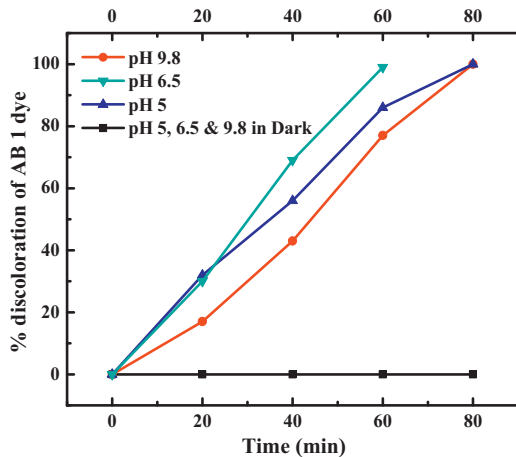


Fig. 9. Effect of solution pH on AB 1 dye degradation using PU-40% SiO₂/TiO₂ hybrid composite film.

loading in hybrid film is related to the increased light scattering by catalyst particles at higher concentration of 70 wt% as these particles may become aggregates at higher concentration to inhibit the dye from contact with the photocatalyst spheres. For the degradation of AB 1 dye under these experimental conditions, the optimum content of catalyst particle in PU-SiO₂/TiO₂ hybrid film was found to be 40 wt% of SiO₂/TiO₂ sphere.

3.4. Effect of pH

Effect of pH on the photodegradation of AB 1 dye for 40 wt% SiO₂/TiO₂ sphere in PU-SiO₂/TiO₂ film was investigated at initial pH of 5, 6.5, and 9.8, as shown in Fig. 9. It was found that the degradation of dye strongly depends on the solution pH (Fig. 9). The removal rate of dye in the solution increased from acidic to neutral pH whereas a decreasing removal rate was observed for the basic dye solution. The point of zero charge (PzC) for TiO₂ was reported as ≈ 6.8 [32]. The TiO₂ surface is positively charged when the pH is below 6.8 and it is negatively charged, the pH is above 6.8. Since, there are two sulfonic acid groups present in the dye and it exists as negative ions in the pH range 5–7 [33]. In the range of pH 5–7, the electrostatic attraction between positively charged TiO₂ in SiO₂/TiO₂-PU and negatively charged dye solution may lead to get the strong interaction between dye and TiO₂ surface in SiO₂/TiO₂-PU. This enables the reaction on catalyst surface that leads to achieve the higher

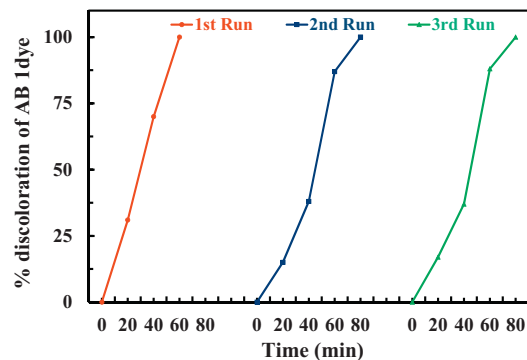


Fig. 10. Reusability of PU-40% SiO₂/TiO₂ hybrid composite film.

degradation in the pH 5–7. Since PU is chemically resistant to acid and alkali, the dissolution of polymer does not occur both in acidic and basic solutions. Therefore, our PU-SiO₂/TiO₂ hybrid composite film could be used as industrial catalyst for effective treatment of dye effluents.

3.5. Reusability test

Reusability of the photocatalyst hybrid film was tested by the degradation of same dye with the used catalyst film. After complete degradation of each run, the PU-40% SiO₂/TiO₂ film catalyst was taken away and washed with deionized water for several times followed by methanol cleaning. The catalyst was dried in a vacuum oven at 80 °C for 12 h and used for next run. Three runs were carried out with the used film catalyst, as shown in Fig. 10. There was little change in the efficiency and catalyst exhibited almost similar degradation ability in the second and third cycles under the same conditions. Hence PU-SiO₂/TiO₂ hybrid composite film could be stable and reusable under UV light.

The advantage of using large amount of SiO₂/TiO₂ composite sphere in the PU matrix is to allow the UV light easily reaching the surface of TiO₂ to enhance the photocatalytical reaction. Although a high weight ratio of composite particle is added, the PU prepolymer solution retains its flowability due to the use of submicrometer-sized SiO₂/TiO₂ particle instead of nanoparticle. To keep TiO₂ to have the photocatalysis performance of nanoparticle, a porous TiO₂ thin layer due to the addition of dodecane during its formation is coated on porous SiO₂ sphere. In this way, the submicrometer-sized SiO₂ particle is loaded with a nano-sized TiO₂ layer to reduce the recombination of photogenerated electron-hole pair [12]. The role of PU is to connect each particle to form the stable film without affecting the photocatalytic effect as well as to control the leaching of SiO₂/TiO₂ composite sphere. Though the concentration of TiO₂ in the PU-40 wt% SiO₂/TiO₂ hybrid film is only 2.6 wt% it has achieved a very good photocatalytic activity. After the success in the reusability of film catalyst without leaching, the PU-SiO₂/TiO₂ hybrid composite film demonstrates an approach to incorporate the functional nanoparticle into polymer matrix, while still keeps the individual characters.

4. Conclusions

Flexible PU-SiO₂/TiO₂ hybrid composite film was fabricated by a simple method and characterized. XRD results revealed the presence of the anatase phase of TiO₂ in the SiO₂/TiO₂ composite sphere. TEM images showed that the SiO₂ sphere and SiO₂/TiO₂ composite sphere were uniform in size without large aggregation and the TiO₂ shell was not broken after annealed at 450 °C. The cross-sectional FE-SEM image showed that SiO₂/TiO₂ composite sphere is evenly distributed in the PU matrix. TGA result of

PU-SiO₂/TiO₂ hybrid composite film showed that SiO₂/TiO₂ composite sphere incorporated into PU matrix increased the thermal stability and degradation temperature. The PU-SiO₂/TiO₂ hybrid composite film showed excellent photocatalytic activity in degradation of Acid Black 1 under UV-light irradiation. The advantage of forming chemical bonding between SiO₂/TiO₂ composite sphere and polyurethane is to avoid the leaching of SiO₂/TiO₂ composite sphere from polyurethane. Flexible PU-SiO₂/TiO₂ hybrid composite film was found to be stable and reusable without appreciable loss of catalytic activity up to three runs. The good performance in photodegradation is related to the PU matrix incorporated with a large amount of submicrometer-sized and porous SiO₂ sphere, on which nano-sized TiO₂ with excellent photocatalytic acitivity locates.

Acknowledgment

This work was supported by NTUST through the grant number of 102H451201.

Appendix A. Supplementary data

Supplementary data associated with this article can be found, in the online version, at <http://dx.doi.org/10.1016/j.apcata.2014.01.044>.

References

- [1] O.I. Alex, F. Paul, *Catalysts* 3 (2013) 189–218.
- [2] U.I. Gaya, A.H. Abdullah, *J. Photochem. Photobiol. C* 9 (2008) 1–12.
- [3] T. Tseng, Y.S. Lin, Y.J. Chen, H. Chu, *Int. J. Mol. Sci.* 11 (2010) 2336–2361.
- [4] K. Hashimoto, H. Irie, A. Fujishima, *Jpn. J. Appl. Phys.* 44 (2005) 8269–8285.
- [5] G. Liu, L.C. Yin, J. Wang, P. Niu, C. Zhen, Y. Xie, H.M. Cheng, *Energy Environ. Sci.* 5 (2012) 9603–9610.
- [6] J. Krysa, G. Waldner, H. Mestankova, J. Jirkovsky, G. Grabner, *Appl. Catal.* 64 (2006) 290–301.
- [7] J. Nisar, Z. Topalian, A.D. Sarkar, L. Osterlund, R. Ahuja, *ACS Appl. Mater. Interfaces* 5 (2013) 8516–8522.
- [8] W.C. Tian, Y.H. Ho, C.H. Chen, C.Y. Kuo, *Sensors* 13 (2013) 865–874.
- [9] M. Stefk, F.J. Heiligtag, M. Niederberger, M. Grätzel, *ACS Nano* 7 (2013) 8981–8989.
- [10] A.S. Nair, P. Zhu, V.J. Babu, S. Yang, T. Krishnamoorthy, R. Murugan, S. Peng, S. Ramakrishna, *Langmuir* 28 (2012) 6202–6206.
- [11] E.J. Villar, V. Mestre, P.C.D. Oliveirab, G.F.D. Sac, *Nanoscale* 5 (2013) 12512–12517.
- [12] C. Liu, D. Yang, Y. Jiao, Y. Tian, Y. Wang, Z. Jiang, *ACS Appl. Mater. Interfaces* 5 (2013) 3824–3832.
- [13] R. Fateh, R. Dillert, D. Bahnemann, *Langmuir* 29 (2013) 3730–3739.
- [14] X. Li, J. He, *ACS Appl. Mater. Interfaces* 5 (2013) 5282–5290.
- [15] P. Wilhelm, D. Stephan, *J. Photochem. Photobiol. A* 185 (2007) 19–25.
- [16] G. Li, R. Bai, X.S. Zhao, *Ind. Eng. Chem. Res.* 47 (2008) 8228–8232.
- [17] S. Singh, H. Mahalingam, P.K. Singh, *Appl. Catal. A* 462–463 (2013) 178–195.
- [18] J. Zhang, F.H.J. Maurer, M. Yang, *J. Phys. Chem. C* 115 (2011) 10431–10441.
- [19] X. Meng, N. Luo, S. Cao, S. Zhang, M. Yang, X. Hu, *Mater. Lett.* 63 (2009) 1401–1403.
- [20] S. Yao, J. Li, Z. Shi, *Particuology* 8 (2010) 272–278.
- [21] S. Matsuzawa, C. Maneerat, Y. Hayata, T. Hirakawa, N. Negishi, T. Sano, *Appl. Catal. B* 83 (2008) 39–45.
- [22] S.N. Hosseini, S.M. Borghei, M. Vossoughi, N. Taghavinia, *Appl. Catal. B* 74 (2007) 53–62.
- [23] P. Lei, F. Wang, X. Gao, Y. Ding, S. Zhang, J. Zhao, S. Liu, M. Yang, *J. Hazard. Mater.* 227–228 (2002) 185–194.
- [24] J. Li, L. Zhu, Y. Wu, Y. Harima, A. Zhang, H. Tang, *Polymer* 47 (2006) 7361–7367.
- [25] T. Yuranova, R. Mosteo, J. Bandara, D. Laub, J. Kiwi, *J. Mol. Catal. A: Chem.* 244 (2006) 160–167.
- [26] P.A. Carneiro, R.F. Pupo Nogueira, M.V.B. Zanoni, *Dyes Pigments* 74 (2007) 127–132.
- [27] J. Paul, K.P. Rawat, K.S.S. Sarma, S. Sabharwal, *Appl. Radiat. Isot.* 69 (2011) 982–987.
- [28] B. Krishnakumar, B. Subash, M. Swaminathan, *Sep. Purif. Technol.* 85 (2012) 35–44.
- [29] B. Subash, B. Krishnakumar, R. Velmurugan, M. Swaminathan, M. Shanthi, *Catal. Sci. Technol.* 2 (2012) 2319–2326.
- [30] B. Subash, B. Krishnakumar, M. Swaminathan, M. Shanthi, *Langmuir* 29 (2013) 29939–29949.
- [31] B. Krishnakumar, M. Swaminathan, *Desalin. Water Treat.* 51/34–36 (2013) 6572–6579.
- [32] I.A. Alaton, I.A. Balcioglu, D.W. Bahnemann, *Water Res.* 36 (2002) 1143–1154.
- [33] B. Krishnakumar, K. Selvam, R. Velmurugan, M. Swaminathan, *Desalin. Water Treat.* 24 (2010) 132–139.